Efficient 3D City Modelling from Airborne Laser Scanning point clouds

GSN Perera# and N Hetti Arachchige
Faculty of Geomatics, Sabaragamuwa University of Sri Lanka, Belihuloya, Sri Lanka
#sanka@geo.sab.ac.lk

Abstract— *Geometrically and topologically correct 3D building models are required to satisfy the increasing demand in, for instance virtual reality, emergency response, robot navigation, and urban planning. Airborne Laser Scanning (ALS) is still the preferred data acquisition system for automated building modelling. In this study, a novel approach for the generation of 3D roof boundaries in Airborne Laser scanner data is presented. The workflow is commenced by segmenting the point cloud which is followed by a classification step and a rule based roof extraction step. Boundary points of the connected roof planes are extracted and fitted straight line segments. We introduce the usage of graph cycles for maintaining the correct topology and optimising the roof reconstruction. Ridge-lines and step-edges are mainly extracted to recognise correct topological relationships among the roof faces. Inner roof corners are geometrically fitted based on the closed cycles. Outer boundary is reconstructed using the same concept but with the outer most cycle. In here, union of the sub cycles is taken. Intermediate line segments are intersected to reconstruct the roof eave lines. Performance analysis of the test results is provided to demonstrate the applicability of the method. The method is further evaluated with the ISPRS benchmark test data and results prove the applicability and robustness of the approach.*

Keywords— *3D Roof Reconstruction, Cycle Graphs, Regularisation, Airborne Laser Scanning*

I. INTRODUCTION

Automated 3D building modeling is important for many applications such as urban planning, virtual reality, environmental studies, telecommunication, 3D Cadastre, emergency response, robot navigation and so on (Brenner, 2005). Currently, point clouds captured by Airborne Laser Scanning (ALS) are basically used in the modeling schemes because they have more automation potential though the points are irregularly distributed. To date, many reconstruction strategies have been developed (e.g. Maas and Vosselman, 1999; Brenner and Haala, 1998; Schwalbe et al., 2005; Oude Elberink, 2010) for the reconstruction of the building models. However, the state-of-art-of-3D-building reconstruction is still being developed, especially, in terms of the efficiency and completeness. In this end, manipulation of roof topology and the way of incorporating roof primitive features are necessary to further experiment in order to reconstruct geometrically valid detailed polyhedral models in a rapid manner. Thus, the objective of this paper is to present a novel approach to make use of topological property of building roof segments and then to reconstruct 3D building roof structures. For this purpose we introduce innovated cycle graph approach.

Initially, raw point cloud is segmented into planar faces and classified as terrain and off-terrain segments. Valid roof planes are extracted afterwards. Roof modeling is then performed based on the cycle graph approach with some geometric constraints. We fit roof corners, by extracting the information from the data, in a valid manner based on the graph cycles. The selection of proper corner features to be intersected and the nature of the convergence are given by the graph cycles.

II. RELATED WORK

Building reconstruction based on the intersection of neighbouring planes, proposed by Maas and Vosselman, (1999), provides the firm basement for many modelling schemes as both data driven and model driven approaches can be linked with the information of intersection edges or ridgelines. Also, Vosselman (1999) and Rottensteiner and Briese (2003) show the validity of the plane intersection method for the modelling schemes. Later on, (Schwalbe et al., 2005) adopt specific orthogonal point projection strategy for the reconstruction workflow. The potential of intersection lines and more comprehensive step-edges to the reconstruction steps is then shown by the (Rottensteiner et al, 2005). Currently, plane intersection information and as well as topological information are being used for the building reconstruction.

Topological information provides the mutual arrangement and/or relationship between neighbouring roof planes. In (2000) Ameri and Fritsch use Voroni diagrams to obtain the mutual connections between the roof planes. Later, (Verma et al., 2006) adopt the

properties of primitive roof shapes by means of the topology. In this approach, it is assumed that any complex building can be decomposed into number of primitive shapes thus the counter recognition of neighbouring primitive is the way to model a building for them. Hence, they recognize the topological relationships among neighbouring roofs of a building and represent in a graph. Consequently, sub graph matching is adopted to detect best possible primitive shape to be represented for a set of roof planes. Although ambiguity of the graph matching has been avoided into certain extent, their approach was limited to a few primitive shapes. After that, formal grammar is added to the primitive shapes that have been identified by sub graph matching by (Milde et al., 2008). In addition to the grammar rules, some additional corner connectors have also been used to get a valid roof model. Sub graph matching, introduced by (Verma et al., 2006), is extended by (Oude Elberink, 2010), and used not only various roof primitive types but also the nature of discontinuity changes among roof planes, i.e. status of ridge-line or step-edge lines, for the matching process. Complete matching result, with few incomplete matches, is obtained from some buildings where missing planes are existed. Thus, incomplete matches is attempted to solve by suggesting a best matched option due to the fact that has been arose as a result of the missing data.

Due to the ambiguities of sub graph matching with relevant data features and limitations of defining possible primitive shapes for the matching, we propose a new approach using cycle graphs. Herein, inner and outer roof boundary lines are reconstructed without recognition of the primitive shapes.

III. ROOF PLANE EXTRACTION

ALS points cloud is initially segmented into different planar faces using seed surface generation by 3D Hough transformation and subsequent surface growing by planar fitting (Vosselman, 2012). Rule based extraction strategy is followed for the detection of roof planes as we do not have any clue about the potential building areas. Accordingly, terrain point classification is a prerequisite, which we need to satisfy prior to the roof extraction. Having planar segments, an extended version of a segment based classification process presented by Perera (2007) is adopted for the extraction of terrain points. Segment adjacencies are first recognized and discontinuities among the segments are then identified along the segment boundaries. This then leads to classify segments as either terrain or off-terrain. Although, we achieve a good classification results, the terrain point classification is not fully discussed here as it is out of scope of the paper.

Assuming, any complex roof can be recognized by detecting their primitive shapes such as gable, hip and so on, different rules are imposed to detect as much of roof segments based on the recognized segment adjacencies. Except isolated flat and shed roofs, most of the other common roofs or part of the roofs might associate with break lines and also individual roof plane might have a certain azimuth difference with respect to the azimuth of the adjacent roof plane. Hence, taking pair of adjacent segments at a time, relative azimuth differences are tested. When the azimuth difference is equal near to the 180 or 0 degree, segments which follow our horizontality constraint on ridge-line is used to refine potential roof planes. Moreover, 90 degree azimuth constraint together with oblique ridge-lines constraint is also used to extract some other roof planes. Further to that, oblique roofs, which have not followed our defined azimuth constraints at their given adjacencies and remained adjacent to the previously detected faces, are extracted using the slope constraints. A height threshold well above the terrain is always imposed to reduce the low vegetation being depicted as roof planes. Summary of the parameters that have been adopted for roof plane extraction is given in Table 1.

Table 1: Summary of the parameter for rules on the roof extraction

Nature of the constraint	Threshold
Azimuth threshold for a roof pair	±3°
Horizontality of break line	< 3°
Slope constraint for oblique roofs	> 5° and < 75°
Slope constraint for the flat roofs	< 5°
Height threshold	1.5 meter

IV. STRATEGY

A. Roof Topology Graph

In general, inner bounds of a roof are mainly given by the ridge-lines and/or step-edge lines. The extraction of such features (let's say feature-lines) between the adjacent roof planes provides the required vector data for inner boundary of building model. Simultaneously, the information can be used to identify correct topological relationships among roof planes which we can later apply for the reconstruction of the outer bounds as well. (Oude Elberink and Vosselman, 2009; Verma et al., 2006) have shown a way of utilizing topological information in a form of a graph called roof topology graph. Similarly, we create roof topology graph while extracting the feature-lines.

C. Closed Cycle Analysis

Assuming the G (see figure 1) as a directed graph, different paths can be chosen for given any two end-vertices. For example, for the end-vertices 3 & 2, possible

sets of vertices are; P1{3,2}, P2{3,4,2}, P3{3,4,6,10,1,2} and so on. If the starting node becomes the end node, then a path will be a (closed) cycle, having a certain "length" (P^k, where k is the length). As such, above paths will become cycles C1, C2 and C3 such that C1={3,2,3}, C2={3,4,2,3} and C3={3,4,6,10,1,2,3}.

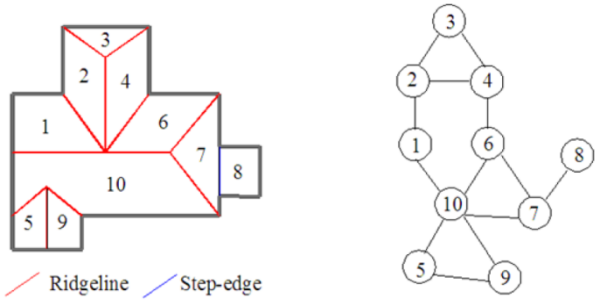

Figure 1: A complex roof structure (left) and its RTG, G (right)

Considering the shortest path problem, cycles having higher degree of lengths can be disregarded while avoiding $p^k \leq 2$ and a unique 'shortest' cycle can be obtained for the given two end-vertices. Thus, the well-known Dijkstra's algorithm (Diestel, 2010) is applied to recognize every possible 'shortest' cycle that appears in a complete RTG. Finally, each RTG is decomposed into possible shortest cycles having varying lengths which can be analyzed individually.

V. MODEL RECONSTRUCTION

A. Fixing of Ridge-line Intersection

Careful examination of Figure 1 shows that the feature lines, relevant to each shortest cycle, are converged to a single point. This means, incidences where the adjacent ridge-lines are supposed to intersect at a single position can be robustly determined by considering every shortest cycle. In this case, as we focus only the ridge-lines, the cycles whose entire edge labels are represented only by the 'ridge-line' category should be chosen. The fixing of such a point can be taken as a least square minimization problem and can be estimated a single position which is closest to all the ridge-lines. We have taken a robust outcome by assigning a weight, which is directly proportional to the sine value of angle between normal vectors of roof segments, for each ridge-line as some ridge-lines are more stable than other (Perera et al., 2012). Therefore, without knowing primitive roof types, ridge-lines can be geometrically fixed as shown in Figure 2.

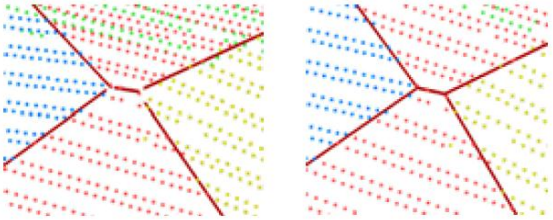

Figure 2: Fixing of ridge-lines supposed to intersect: before (left), after fixing (right)

B. Fixing Relevant to Step-edges

In addition to the ridge-line intersection, many possibilities can be found where step-edge lines (themselves) and step-edge with ridge-lines suppose to be converged at more than one positions (see, Figure 3), holding a same planimetric coordinates with height jumps. Therefore, by analyzing the feature lines together with shortest cycles, at a 3D view, a single common position is constructed. However, presence of step-edges split the 'cycle' into several 'arcs'. Each arc represents a specific height level of the roof top. As two height levels exist in the Figure 3(middle), two arcs or two directed "path graphs" can be used to represent that shortest cycle. The splitting of cycles lead to convey in which step edge i.e. either up or down edge, is referred by the particular path graph. Consequently, all the feature lines, relevant to a certain path graph can be identified, and computed a single intersection point (3D) to represent the corresponding roof corner. However, due to the other path graphs, exist in the same cycle; slightly different planimetric coordinates might be received. Thus, a common planimetric position is taken by averaging each individual position. Transferring of the planimetric coordinate to the other points leads for the geometrically valid roof corners.

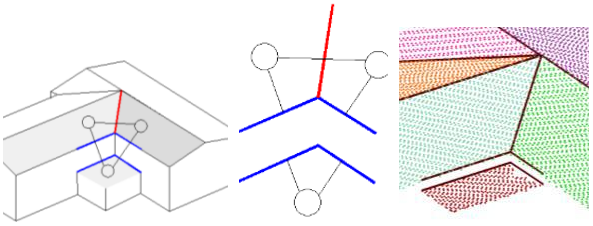

Figure 3: Convergence of step-edges and ridge-lines. (left) with the cycle, (middle) disjoint paths, (right) after corner fixing

During the adjustment process, step-edges are allowed to shift while preserving their directions based on the influence of ridge-lines since the ridge-lines are fixed in our approach.

D. Fixing of Outer Bounds

Outer bounds are defined by extracting boundary points. For this, outer contour of the connected components are first obtained. This then decomposes in to corresponding laser segments. In order to represent gutters and eaves, rectilinear line segments are fitted for boundary points corresponded to each contour segment. Each line segment is regularized by introducing an angle threshold to the dominant building direction. Still outer bounds are not coincided with inner skeleton to make closed polygons. Therefore, outer ends of the inner skeleton are fixed with the outer boundary line segments using outer most closed cycle of the RTG.

For the graph G in Figure 1, the outer most cycle can be obtained by taking union of all the sub cycles and the path of the outer cycle can be written with vertices in the order of { 1,3,4,3,2,6,5,2,7,1}. In this case, end-vertex is equal to the vertex 1. Normally, at a roof corner, two outer boundary line segments and an inner boundary line segment (i.e. a feature line) converge to a single position to make a corner position in 3D. As such, forward traversing along the outer cycle will lead to fix necessary (outer) roof corners by intersecting respective feature line and outer boundary line segments. When two intersection points are existed at a feature line, then most outer point is chosen in order to compensate the size changes of the building foot print. Remaining intermediate outer boundary line segments are then intersected sequentially in order to obtain intermediate turning points in eaves or gutter edges. Geometrically correct valid 3D roof models are ultimately achieved as shown in Figure 4.

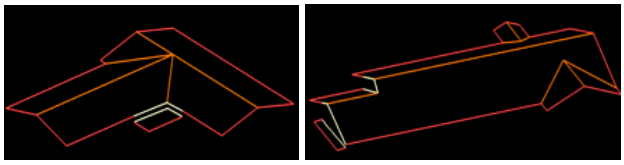

Figure 4: Reconstructed complex roof models. red – outer bounds, orange – ridge-lines, white – step-edges

E. Reconstruction of Wall Segments

The height beneath the roof model, along the roof outer boundary, is extracted from the laser segments. The lowest terrain height is taken as the basement of the corresponding building. Down projecting the roof outer boundary points (vertices) until the defined basement, each wall segment is reconstructed (e.g. Figure 5). Figure 5 further reveals the entire building models of the test site.

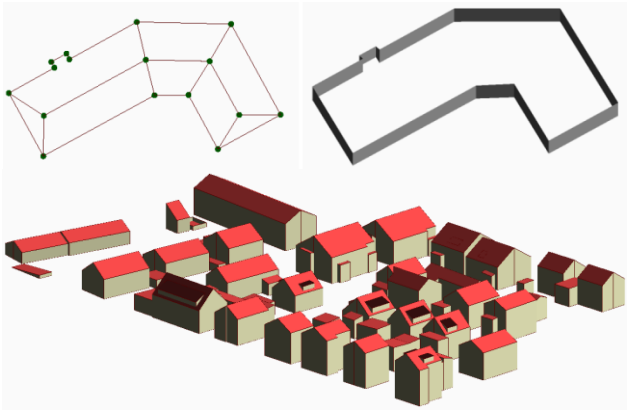

Figure 5: Reconstruction of building walls and final 3D buildings: (top-left) roof vertices; (top-right) reconstructed wall segments; (bottom) reconstructed 3D building models

VI. EXPERIMENT AND ANALYSIS

In this section, we present the performance and limitations of our proposed algorithm, in both quantitative and qualitative terms. The accuracy of 3D roof models is also analysed in the context of the ISPRS WG III/4 ''Test Project on Urban Classification and 3D Building Reconstruction'', which allows us to use external reference data. One test scene located in Vaihingen, Germany, provided by ISPRS Com. III WG III/4, was used for the purpose of this paper. The test site is a purely residential area having small detached houses.

A. Performance of Cycle Approach

A quantitative assessment for cycle analysis has been conducted manually by comparing statistics estimated from the reconstructed models with the corresponding aerial imageries. Table 2 summarises the evaluation of both inner- and outer boundaries fixed by the cycle analysis. It shows that 57% (9 out of 16) of the inner roof corners are correctly fixed by the approach, whereas the achieved modelling performance (MP) is 67% (103 out of 155). The MP is calculated as the ratio of CP to TOT. CP and TOT are interactively counted by superimposing results on image data. The main reason for the low performance rate is misclassification of some roof segments. The absolute figures of MP, comparatively, illustrate a high performance (95% = 103 out of 109). The objective of computing the absolute figures is to estimate the negative contribution done by the cycle analysis approach exclusively. Higher absolute figures further reveal the robustness of the closed cycle analysis for fixing inner-boundaries. In contrast to correct fixings, there are few incorrect fixings mainly because of the absence of small roof segments, mismatch of parameters or over/under-segmentation. In fact, the absence of

segments can lead to a lack of graph edges, and the resultant distorted cycles can cause fault geometry.

Table 2: Summary of cycle analysis

Nature	Overall (based on existing roofs)	Absolute (based on CE)
# Extractable inner cycles	16	9
# Correctly fixed inner cycles	9	9
# Wrongly fixed inner cycles	0	0
# Missed inner cycles	7	0
# Geometrically acceptable closed polygon (CP)	103	103
# Partially correct closed polygon	6	6
# available total polygon (TOT)	155	109
Modelling performance – polygon (MP)	65%	94%

B. Evaluation of Geometrical Accuracy

During the quality analysis, the orthogonal distance between model planes and laser points can be used as a quality measure. Dorninger and Pfeifer (2008) and Oude Elberink and Vosselman (2011) also used it as a segmentation quality measure in the absence of reference data. We compute the rmse between model planes and laser points by means of the orthogonal distance. The objective is to measure how final roof models fit laser points as some of the original roof planes are slightly adjusted over the course of ridge-line intersection. Figure 6 shows that model planes fit laser points well as the majority of planes exhibit an rmse less than 0.2 m. Higher errors mainly occur in small roof models such as dormers or garages. In Figure 7, the process maintains the symmetries of most of the gable-shaped roof pairs within ±0.05 m tolerance, although a few buildings deviate largely in the test scene. The deviations are caused by unequal roof inclination or non-symmetry. These deviations can be expected because constraints on inclination are not enforced. Similarly, a correct alignment of gutter positions can easily be achieved even when gutters reside at different height levels (see Figure 8).

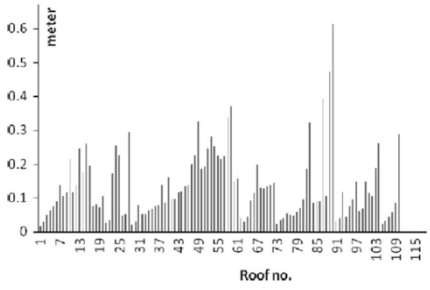

Figure 6: RMS error between model planes and laser points

To analyse the geometric quality of closed polygons, the planimetric deviation of each vertex is computed with the nearest vertex in the reference data and presented in rmsd. Table 3 shows that the mean rmsd is 0.7 m, which is nearly double the point spacing of laser data. The small red and blue regions (Figure 10) can also be used to see how and where over/under-estimation of outer-boundaries occurs.

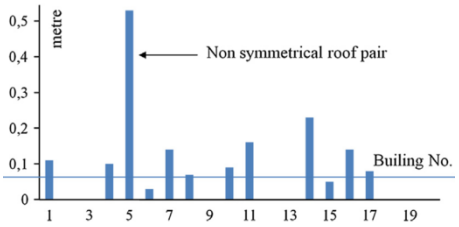

Figure 7: Gutter symmetry of reconstructed roof models

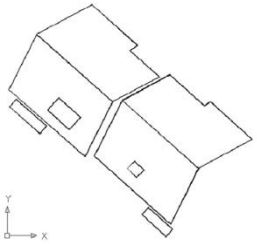

Figure 8: valid gutter alignment at multiple height levels

For the assessment of vertical accuracy, vertical errors in roof models are detected using the height difference between corresponding pixels of the reference DSM. Table 3 and Figure 9 show that we obtain good height accuracy with few large errors where small objects or height jumps exist. Errors close to step-edge locations show the uncertainty of edges (and are thus in fact planimetric errors). This error is not a failure of the cycle approach as it is common for sparsely distributed ALS data.

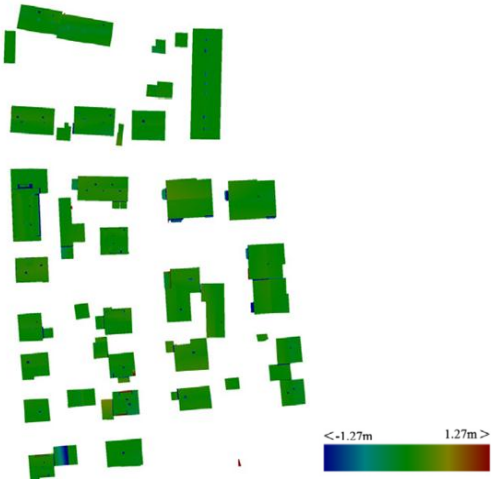

Figure 9: Height errors

C. Overall Evaluation

The overall performance of the roof reconstruction process is reported via three measures, namely (1) completeness, (2) correctness and (3) quality as defined by Rutzinger et al. (2009). Their statistics are shown in Table 3.

Table 3: Overall statistics

Nature of measurer	value
Completeness	74.0
Correctness	93.8
Quality	70.6
Topological deviations	
1:1 / 1:N / M:1 / M:N	63 / 0 / 42 / 1
RMSD (m) planimetry	0.7
RMSZ (m) height	0.1

In general, end products exhibit 94% correctness in terms of roof planes. However, the completeness is fairly low, as almost 25% of the roof planes are missing in our final closed polygons. According to the fluctuations of the first two measures, the quality remains at 71%. Possible error sources for low completeness are over/under-segmentation, misclassification of building segments, incorrect roof plane extraction, and the inability to make closed polygons due to some missing feature lines. Table 3 shows that the quality of extracted building segments are affected by under-segmentation (1:N > M:1). Figure 11 exhibits how correctness, completeness, and quality behave in a roof plane area. The graph shows that the method performs well in terms of large roof planes with all performance measures reaching their peak. In contrast, low completeness is found in small objects with an insufficient number of points.

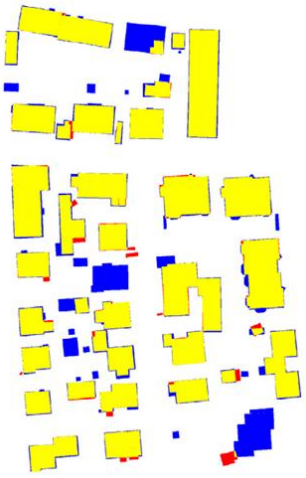

Figure 10: Overall performance of roof reconstruction

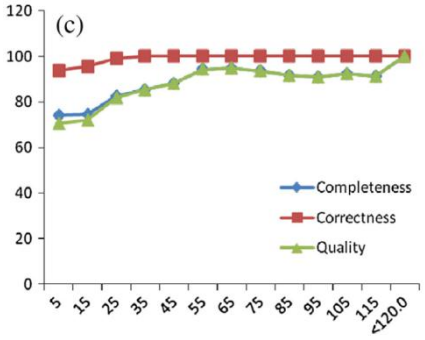

Figure 11: Overall quality of roof models

VII. CONCLUSION

A novel cycle graph strategy, which particularly correlates the convergence of feature lines and outer boundary line segments, is used for model reconstruction. The main advantage of this process is its ability to reconstruct geometrically correct detailed roof models without knowing their primitive shapes. The strategy used to fix outer-boundaries is useful for maintaining gutter symmetries and boundary alignments. It can preserve less than 5 cm symmetrical uncertainty for most roof types. Flat and slant roofs having multi-layer height jumps can also be reconstructed. High modelling performance (MP) demonstrates the robustness of the closed cycle graph concept for roof reconstruction. In spite of low completeness, high correctness has been obtained. The main reason for low completeness is in defects associated with the classification step. Considering polygon geometry, a high geometric accuracy (0.1 m/0.7 m for height and planimetry) is achieved by the process.

Future work will mainly concern further improvements of the process.

ACKNOWLEDGMENT

This research was funded by the German Academic Exchange Program (DAAD). The Vaihingen data set was provided by the German Society for Photogrammetry, Remote Sensing and Geoinformation (DGPF) [Cramer, 2010]:http://www.ifp.uni-stuttgart.de/dgpf/DKEP-Allg.html (in German). The authors wish to thank the chair persons of ISPRS Commission III/4 for providing them with data and evaluating the test results.

REFERENCES

Ameri, B., Fritsch, D., 2000. Automatic 3D building reconstruction using plane-roof structures. In: ASPRS Congress, Washington, DC, pp. 12.

Brenner, C., Haala N., 1998. Fast reality production of Virtual Reality City Models. IAP, Vol. 32, Part 4.

Brenner, C., 2005. Building reconstruction from images and laser scanning. International Journal of Applied Earth Observation and Geoinformation 6 (3), 187–198.

Dorninger, P., Pfeifer, N., 2008. A comprehensive automated 3D approach for building extraction, reconstruction, and regularization from airborne laser scanning point clouds. Sensors 8 (11), 7323-7343.

Diestel, R., 2010. Graph Theory, fourth ed. Springer-Verlag., Heidelberg.

Maas, H.G., Vosselman. G., 1999. Two algorithms for extracting building models from raw laser altimetry data. ISPRS Journal of Photogrammetry and Remote Sensing 54 (2-3), 153-163.

Milde, J., Zhang, Y., Brenner, C., Pluemer, L. Sester, M., 2008. Building reconstruction using a structural description based on a formal grammar. International Archives of Photogrammetry, Remote Sensing and Spatial Information Sciences 37 (Part 3B), 227-232.

Oude Elberink, S. and Vosselman, G., 2009. Building Reconstruction by Target Based Graph Matching on Incomplete Laser Data: Analysis and Limitations. *Sensors*, 9(9): 6101-6118.

Oude Elberink, S., 2010. Acquisition of 3D topography: Automated 3D road and building reconstruction using airborne laser scanner data and topographic maps. Ph.D. dissertation, University of Twente, Enschede, The Netherlands.

Oude Elberink, S., Vosselman, G., 2011. Quality analysis on 3D building models reconstructed from airborne laser scanning data. ISPRS Journal of Photogrammetry and Remote Sensing 66 (2), 157–165.

Perera, G.S.N., 2007. Segment based filtering of LASER scanner data, Master thesis, ITC, The Netherlands.

Perera, G.S.N., Nalani, H.A., Maas, H.-G., 2012. An automated method for 3D roof outline generation and regularization in airborne laser scanner data. ISPRS Annals of the Photogrammetry, Remote Sensing and Spatial Information Sciences 1 (3/W4), 281-286.

Rottensteiner, F., Briese, C., 2003. Automatic generation of building models from lidar data and the integration of aerial images. International Archives of Photogrammetry, Remote Sensing and Spatial Information Sciences 34 (Part 3/W13), 174-180.

Rottensteiner, F., Trinder, J., Clode, S., Kubik, K., 2005. Automated delineation of roof planes from lidar data. International Archives of Photogrammetry, Remote Sensing and Spatial Information Sciences 36 (Part 3/W4), 221-226.

Rutzinger, M., Rottensteiner, F., Pfeifer, N., 2009. A comparison of evaluation techniques for building extraction from airborne laser scanning. IEEE Journal of Selected Topics in Applied Earth Observations & Remote Sensing 2(1), 11-20.

Schwalbe, E., Maas, H.-G., Seidel, F., 2005. 3D building model generation from airborne laser scanner data using 2D GIS data and orthogonal point cloud projections. International Archives of Photogrammetry, Remote Sensing and Spatial Information Sciences 36 (Part 3/W19), 209-213.

Verma, V., Kumar, R. Hsu, S., 2006. 3D building detection and modeling from aerial lidar data. In: The IEEE Computer Society Conference on Computer Vision and Pattern Recognition, 17-22 June, IEEE Computer Society, Washington, DC, USA, pp. 2213-2220.

Vosselman, G., 1999. Building reconstruction using planar faces in very high density height data. International Archives of Photogrammetry, Remote Sensing and Spatial Information Sciences 32 (Part 3/2W5), 87-92.

Vosselman, G., 2012. Automated planimetric quality control in high accuracy airborne laser scanning surveys. ISPRS Journal of Photogrammetry and Remote Sensing 74, 90-100.

BIOGRAPHY OF AUTHORS

Dr Sanka Perera received his PhD in Remote Sensing and Photogrammetry from Technical University of Dresden, Germany. Currently he is a senior lecturer in the Faculty of Geomatics, Sabaragamuwa University of Sri Lanka. He has developed several algorithms and some new concepts for processing of Point clouds data and his main research interest is to model 3D topography using Airborne Laser Scanner data

Dr Nalani Hetti Arachchige obtained her PhD for the development of a new algorithm for 3D facade modeling from mobile LASER scanner point clouds, from the Technical University of Dresden, Germany. Currently, she is also a senior lecturer in the Faculty of Geomatics.